Supporting Information

Bingwei Zhong,[a,b] Jian Zhang,[c] Bo Li,[b] Bingsen Zhang,[b] Chunli Dai,[b] Xiaoyan Sun,[b] Rui Wang[b] and Dang Sheng Su*[b]*

[a] University of Science and Technology of China, 96 Jinzhai Road, Hefei, 230026, China

[b] Catalytic Materials Division, Shenyang National Laboratory for Materials Science, Institute of Metal Research, Chinese Academy of Sciences 72 Wenhua Road, Shenyang 110016, China. E-mail: dssu@imr.ac.cn

[c] Ningbo Institute of Materials Technology & Engineering, Chinese Academy of Sciences 519 Zhuangshi Road, Ningbo 315201, China. E-mail: jzhang@nimte.ac.cn

Experimental Section

Materials. Two products from Alfa Aesar and Tangshan Guanghua Jingke (China) with different textural properties were used as the representative activated carbons. The single-wall nanotube sample was obtained from Shenzhen Nanotech port Co., Ltd. (China). The multiwall nanotubes sample was obtained from Bayer Material Science Co. (Germany). Nanodiamond (Beijing Grish Hitech Co., China) was synthesized by detonation explosive method followed by acid washing. The ND samples were calcined at 1000, 1100, 1200, 1300, 2000°C in argon for 4 h to vary the sp^2/sp^3, labeled as ND-1000, ND-1100, ND-1200, ND-1300 and ND-2000 which all had onion-like carbon (OLC) structure.

Methane decomposition reaction. The catalysis experiments were carried out in a fixed-bed reactor at atmospheric pressure. The temperature was increased to 850 or 900°C with a ramp of 10 K min^{-1} under a flow of inert N_2. All catalyst with amount of 150 mg was evaluated in a flow of 50 mL min^{-1} of 10% CH_4 in N_2. After reaction, the sample was purged by N_2 and cooled down to the room temperature. In all cases, no product other than hydrogen can be detected. The CH_4 conversion were calculated from Eq. (1), where $F_{CH4;\ IN}$ and $F_{CH4;\ OUT}$ are the initial and final methane flow rates, respectively.

$$X_{CH4} = (F_{CH4;\ IN} - F_{CH4;\ OUT}) / F_{CH4;\ IN} * 100\% \qquad (1)$$

Catalyst characterization. The textural properties of the catalysts were characterized by N_2 physisorption tests, obtained with a Micromeritics ASAP2020 instrument. The surface oxygenated functionalities before and after reaction were characterized by temperature programmed desorption (TPD) using a quartz tube reactor in flowing helium (50 mL min^{-1}) with a heating rate of 10 K min^{-1} from 293 K to 1243 K. The amounts of CO, CO_2, and H_2O desorbed were probed by a quadrupole mass spectrometer. The fourier-transform infrared (FTIR) spectra were obtained on a Thermo Nicolet iS10 infrared spectroscope from 4000 to 400 cm^{-1} by KBr method at room temperature. XPS characterization was performed on an ESCALAB 250 instrument with Al Kα X-rays (1489.6 eV). Transmission electron microscopy (TEM) was used to determine the particle size and morphology of both fresh and used catalysts on a F20 microscope with an accelerating voltage of 200 kV. Static secondary ion mass spectroscopy (SIMS) with a TOF-SIMS V instrument carried out at 500um*500um, 128*128 pixels region with 30 keV electron beam, and the $C_2H_2^-$ peak was normalized by the C_2^- peak.

Computational Setup. The calculations are performed by using periodic, spin-polarized DFT as implemented in Vienna *ab initio* program package (VASP).[1,2] The electron-ion interactions are described by the projector augmented wave (PAW) method proposed by Blöchl[3] and implemented by Kresse[4] PBE functional[5] is used as exchange-correlation functional approximation and a plane wave basis set with an energy cutoff of 400 eV is used. A 6*6 cell of graphene is used in the calculation and a 3*3 k point mesh is for brillouin zone sampling. During structure optimization all atoms in the unit cell are allowed to relax and no symmetry is imposed. The optimization is stopped when the maximum force on the atoms is smaller than 0.02 eV/Å. The distance between neighbouring cells is 10 Å. The reaction barrier is calculated using the climbing image nudged elastic band (CI-NEB) method[6].

1. G. Kresse, J. Furthmüller. *Comput. Matt. Sci.* 1996, **6**, 15-50.

2. G. Kresse, J. Furthmüller. *Phys. Rev. B*. 1996, **54**, 11169-11186.

3. P. E. Blöchl. *Phys. Rev. B*. 1994, **50**, 17953-17979.

4. G. Kresse, D. Joubert. *Phys. Rev. B*. 1999, **59**, 1758-1775.

5. J. P. Perdew, K. Burke, M. Ernzerh. *Phys. Rev. Lett.* 1996, **77**, 3865–3868.

6. G. Henkelman, B. P. Uberuaga, H. Jonsson. *J. Chem. Phys.* 2000, **113**, 9901–9904.

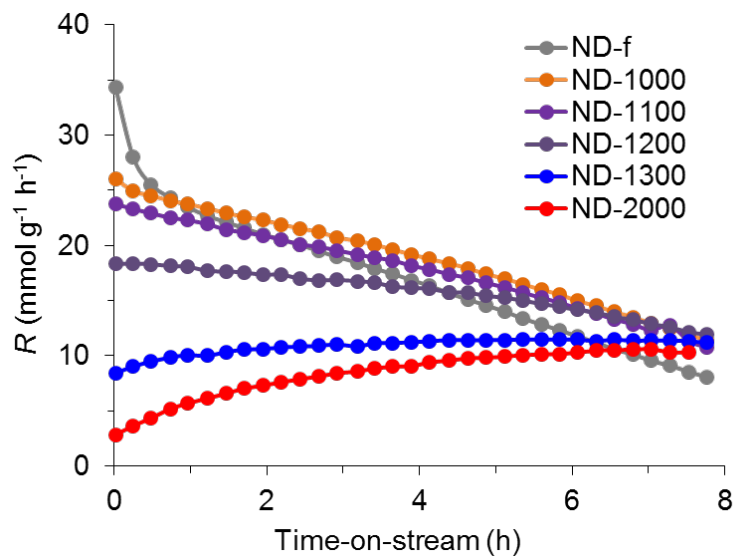**Figure S1.** Performance evaluation of the catalysts on CMD reaction for ND-f and calcined ND samples at 900°C.

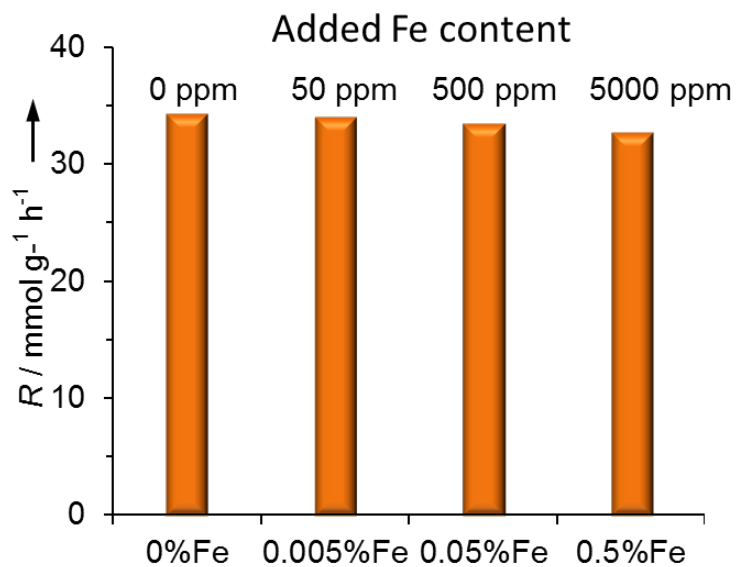

Figure S2. Effect of added Fe on the activity of ND-f.

3

Table S1. Textural properties of the all ND samples before and after reaction.

Catalysts	Before reaction		After reaction	
	BET surface area $(m^2 \, g^{-1})$	Pore Volume $(cm^3 \, g^{-1})$	BET surface area $(m^2 \, g^{-1})$	Pore Volume $(cm^3 \, g^{-1})$
ND-f	313.0	1.266	90.8	0.128
ND-1000	345.0	1.466	88.3	0.135
ND-1100	350.2	1.505	101.2	0.153
ND-1200	364.3	1.532	163.2	0.246
ND-1300	386.3	1.560	307.2	0.543
ND-2000	427.1	1.624	343.2	0.759

Figure S3. In-situ CMD reaction of ND-f catalyst: a, FT-IR; b, TPD; c, Performance evaluation for ND-f before and after 900°C TPD experiment.
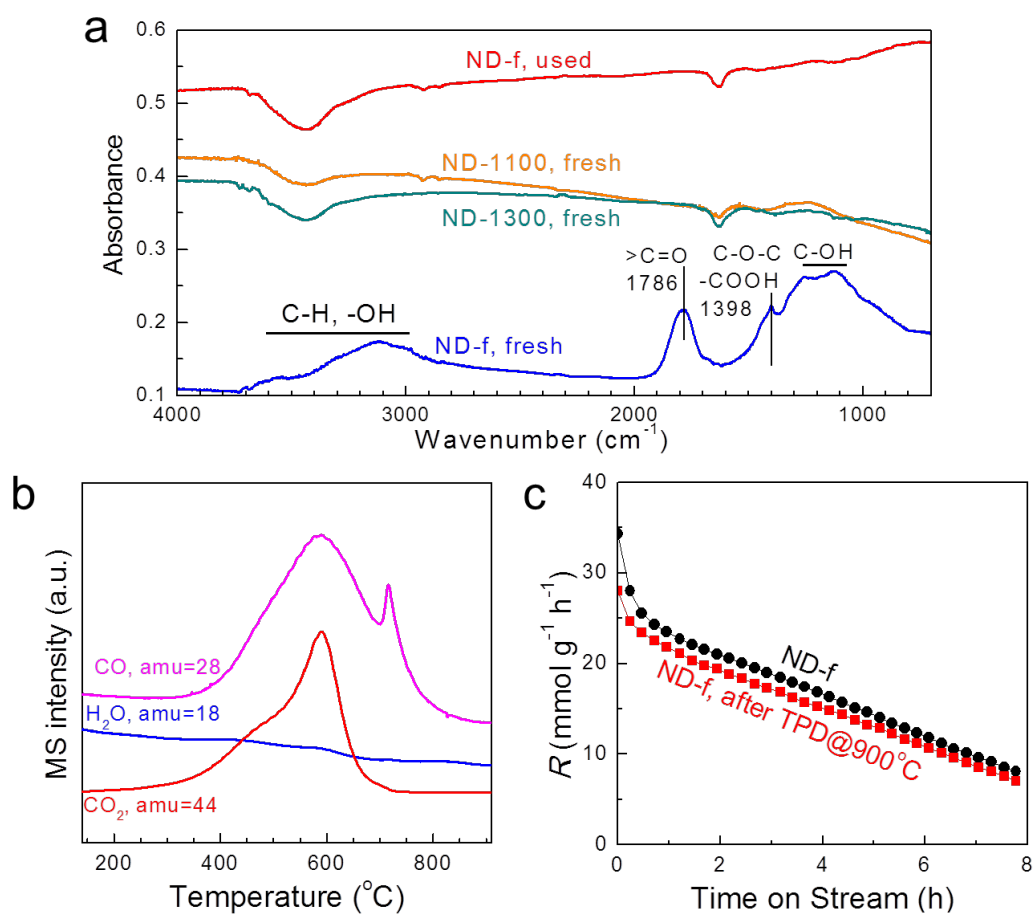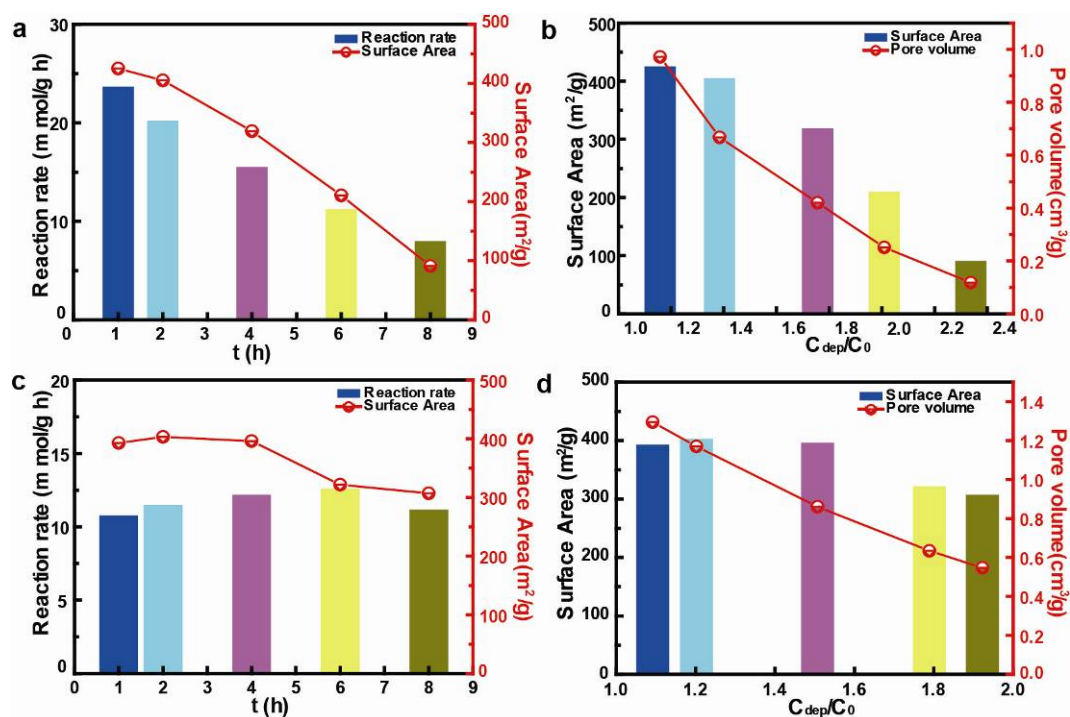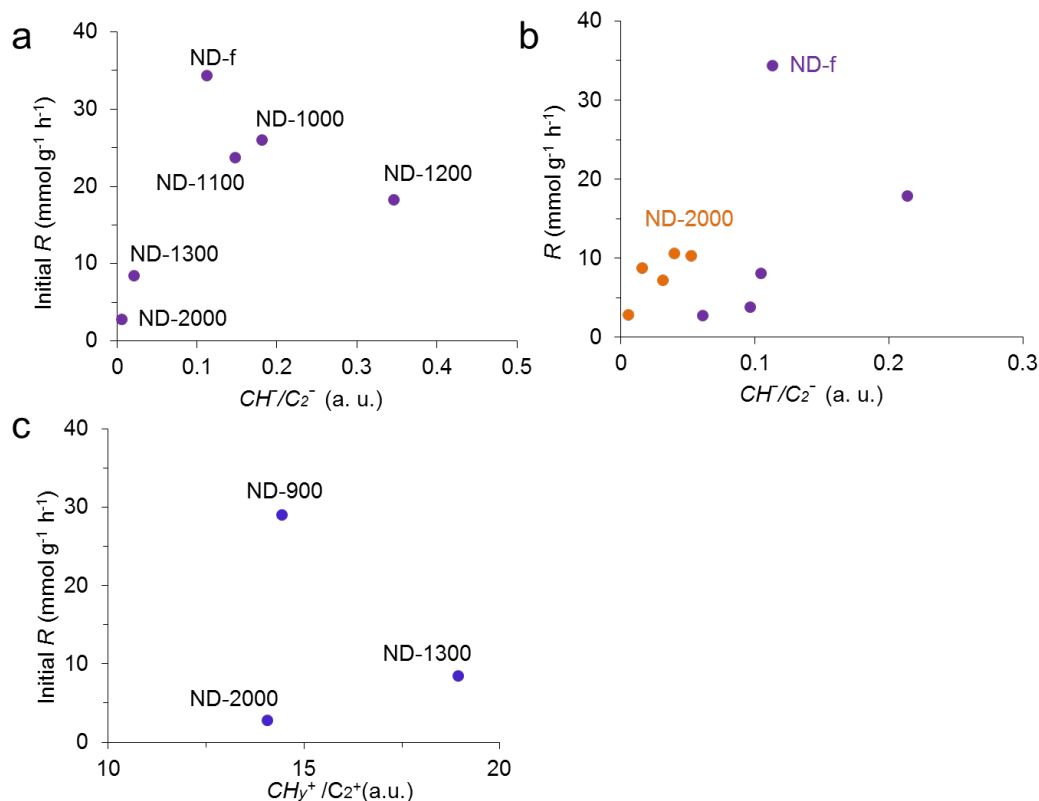

5

Figure S4. Influence of textural properties on the catalytic activity of ND-f and ND-1300 in CMD. ND-f: a, Correlation between CH_4 reaction rate and evolution of the surface area. b, Surface area and total volume of pores vs. deposited carbon with respect to the initial mass of catalyst. C_{dep}/C_0 is defined as the amount of carbon deposits per gram of catalyst. c and d corresponding to ND-1300.

Figurer S5. a, Relationship between CH_4 initial rate and CH^-/C_2^- of NDs, b, Relationship between CH_4 rate and $C_2H_2^-/C_2^-$ of ND-f and ND-2000 at different times on stream, c, Relationship between CH_4 initial rate and CH_y^-/C_2^- of NDs (y=1-3).

As it has been reported in negative SIMS spectra[22], for the same kind material, when the CH^- peak is less intense than C_2H^- peak, the CH^-/C_2^- peak, the most intense signal in the CH_x^- region (x=1,2), reveals the presence of aliphatic groups that the weak CH^- peak corresponds to the low surface concentration of aliphatic compounds. And to positive SIMS spectra[18], the positively charged fragment ions ΣCH_y^+ (y=1-3) fragment ions such as CH^+, CH_2^+, and CH_3^+ can indicate the presence of higher amounts of aliphatic surface compounds. As show in the Figure S4, no clear relationship can be established between the CH_4 rate and CH^-/C_2^-, $\Sigma CH_y^+/C_2^+$ for the NDs. That means the aliphatic groups have no contribution and are impossible as the active sites to the CH_4 decomposition reaction.

Table S2: Results of the XPS and SIMS measurements on the ND catalysts.

Catalyst	Initial R ($mmol\ g^{-1}\ h^{-1}$)	$C_{1s}(eV)$	FWHM (eV)	sp^2/sp^3 (XPS)	$C_2H_2^-/C_2^-$
ND-f	34.3	284.6(34.7%) 286.5(51.2%) 287.4(10.8%) 288.7(3.3%)	1.71	0.68	1.58
ND-1000	26.0	284.3(44.0%) 285.5(26.4%) 286.7(27.5%) 288.0(2.0%)	1.53	1.60	1.23
ND-1100	23.8	284.6(57.2%) 285.9(9.7%) 286.8(33.1%)	1.50	1.73	1.01
ND-1200	13.8	284.4(47.5%) 285.7(24.1%) 286.9(24.9%) 288.9(3.4%)	1.44	1.90	0.66
ND-1300	8.4	284.5(63.7%) 285.4(19.9%) 286.9(14.7%) 290.2(1.7%)	1.25	4.33	0.34
ND-2000	2.8	284.6(57.5%) 285.5(14.2%) 286.7(9.4%) 290.4(19.0%)	1.10	6.14	0.02